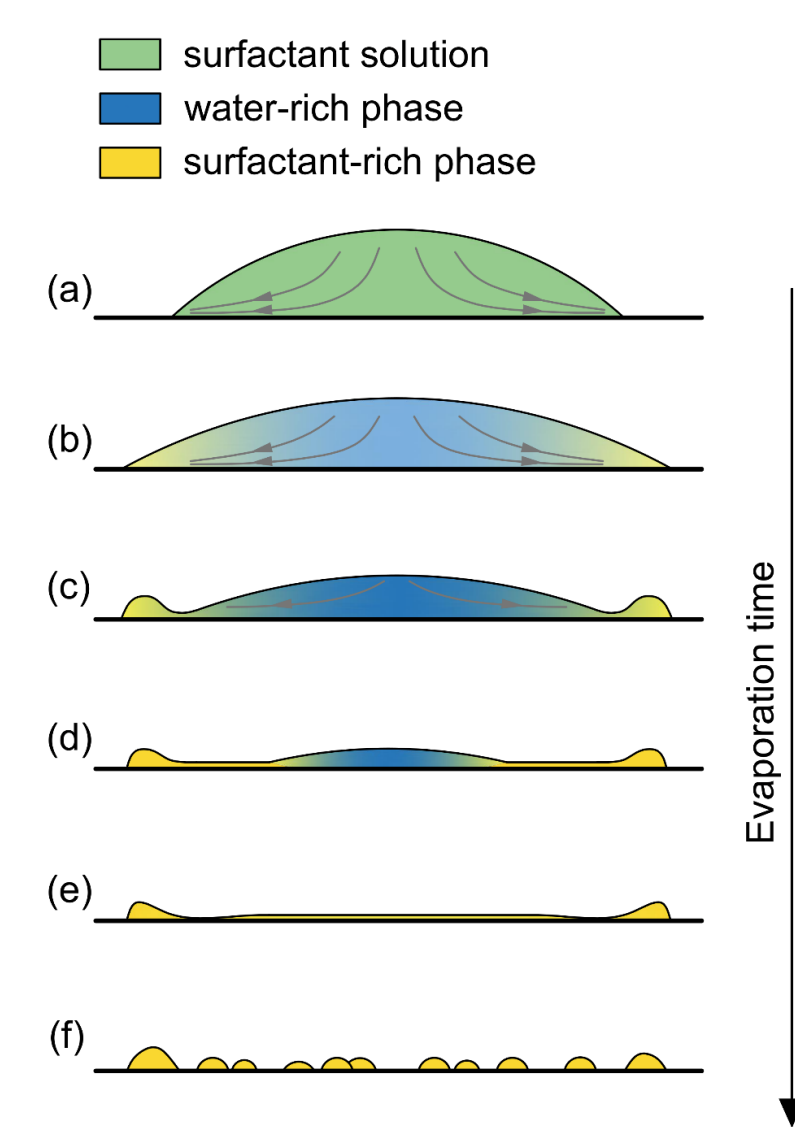


1 Introduction

Surfactant is a versatile chemical in different formulations. Understanding the influence of surfactants on drying droplets is of importance for various industries, e.g., printing, spray coating and agricultural spraying. Drying characteristics of droplets with non-ionic surfactant polyoxyethylene alkyl ethers (C_nE_m) remain scarcely explored though they are widely used as emulsifying agents and detergents.

We studied systematically the wetting and drying behaviours of aqueous pico-litre droplets with C_nE_m and compared with those containing anionic surfactant sodium dodecyl sulfate (SDS). The spreading and drying of surfactant-laden droplets on hydrophilic substrates were studied by three-phase contact line (TCL) tracking and interferometry. We found that a drying C_nE_m -laden droplet distinctively undergoes phase separation — a water-rich droplet retracts and leaves a surfactant mesophase thin film behind. We also found that surprisingly both C_nE_m and SDS solutions inhibit spreading on hydrophilic surfaces, and attributed this phenomenon to Marangoni contraction as a result of surface tension gradient across the gas-liquid interface. More

pronounced suppression of spreading is observed in the case of C_nE_m solutions, which is believed due to phase transition of surfactant solution to mesophase at the vicinity of the initial TCL as droplet spreads and dries simultaneously. Internal flow of droplets is revealed by tracer particles that mild Marangoni flows exist in general for droplets with surfactant concentrations well above critical micelle concentration (CMC).



3 Results

A General picture of the drying process

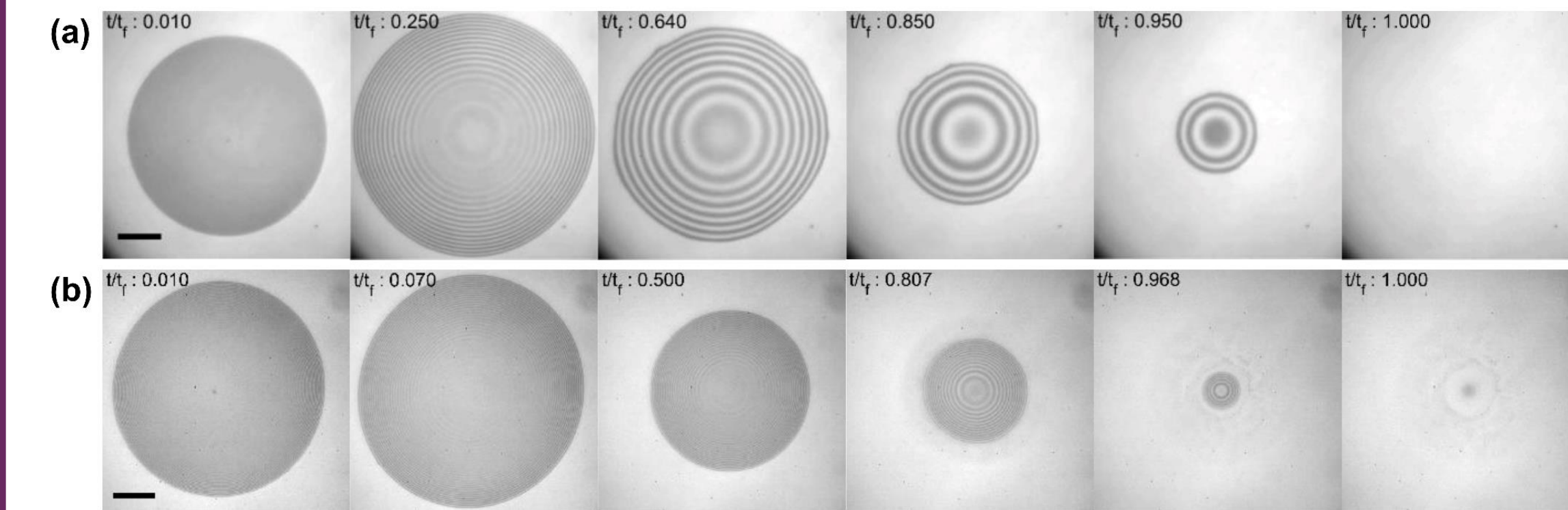


Figure 1. Underneath-view images during the drying of a pure water droplet (a, $t_f=0.98$ s) and a 5mM SDS-laden droplet (b, $t_f=1.28$ s). Scale bars for 50 μm and t_f denotes the vanishing time of a receding droplet.

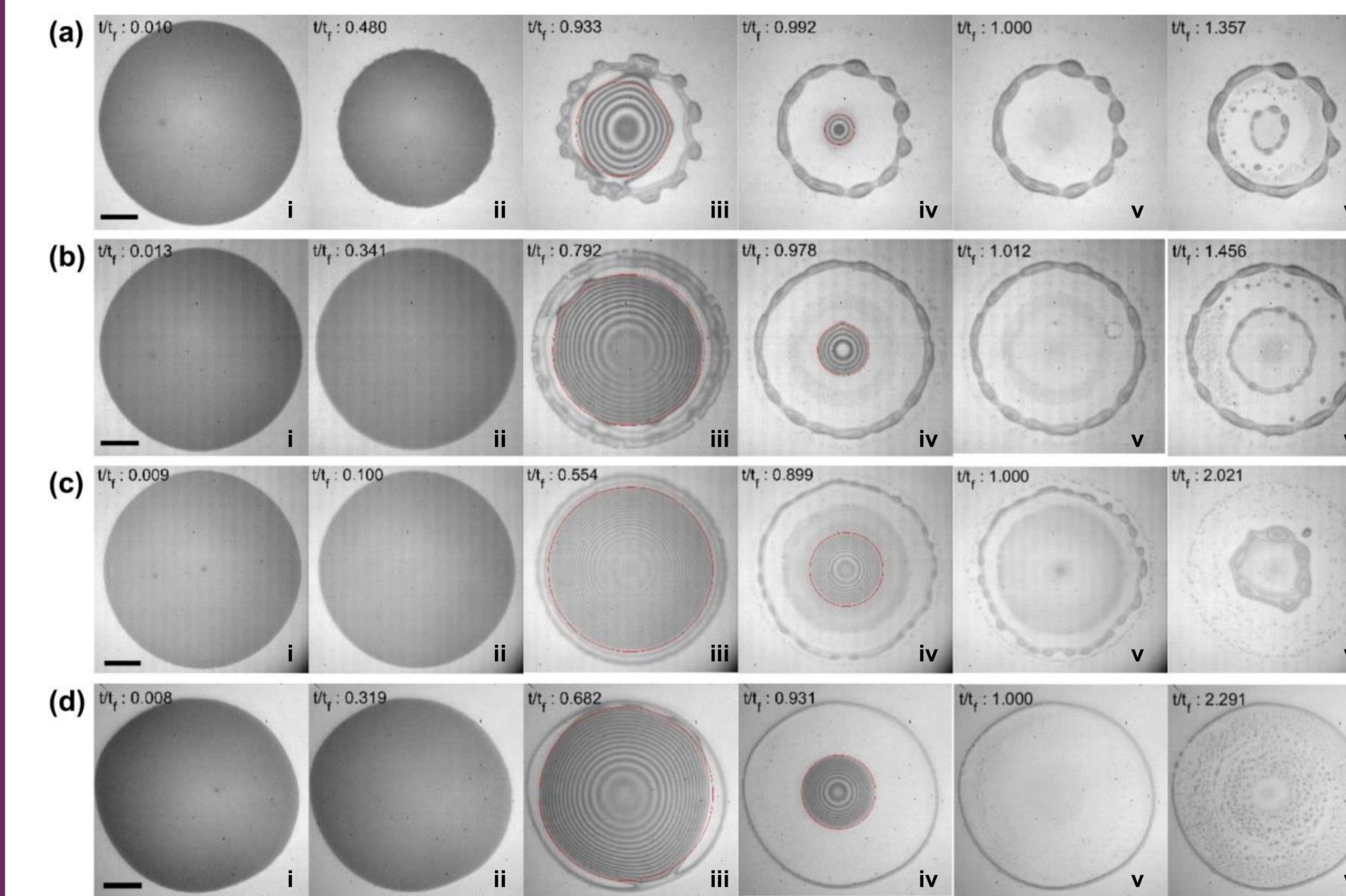


Figure 2. Underneath-view images during the drying of C_nE_m -laden droplets. Scale bars for 50 μm . t_f denotes the vanishing time of a receding water-rich droplet and the red lines illustrate tracked contact lines of the receding droplets. (a) 5 mM $C_{10}E_8$, $t_f=1.71$ s; (b) 5 mM $C_{12}E_8$, $t_f=1.47$ s; (c) 5 mM $C_{14}E_8$, $t_f=1.43$ s; (d) 5 mM $C_{14}E_6$, $t_f=1.08$ s.

- Compared to the simple drying processes of water and SDS-laden droplets, the C_nE_m -laden droplets show complex drying dynamics.
- As a C_nE_m -laden droplet dries, a droplet that contains the major liquid volume continuously retracts until vanishing while leaving a thin film behind. The thin film shows instability which eventually breaks into tiny droplets.
- We attribute the drying behaviours of C_nE_m -laden droplets to phase transition and separation. The retracting droplet is a water-rich phase and the thin film is a mesophase.

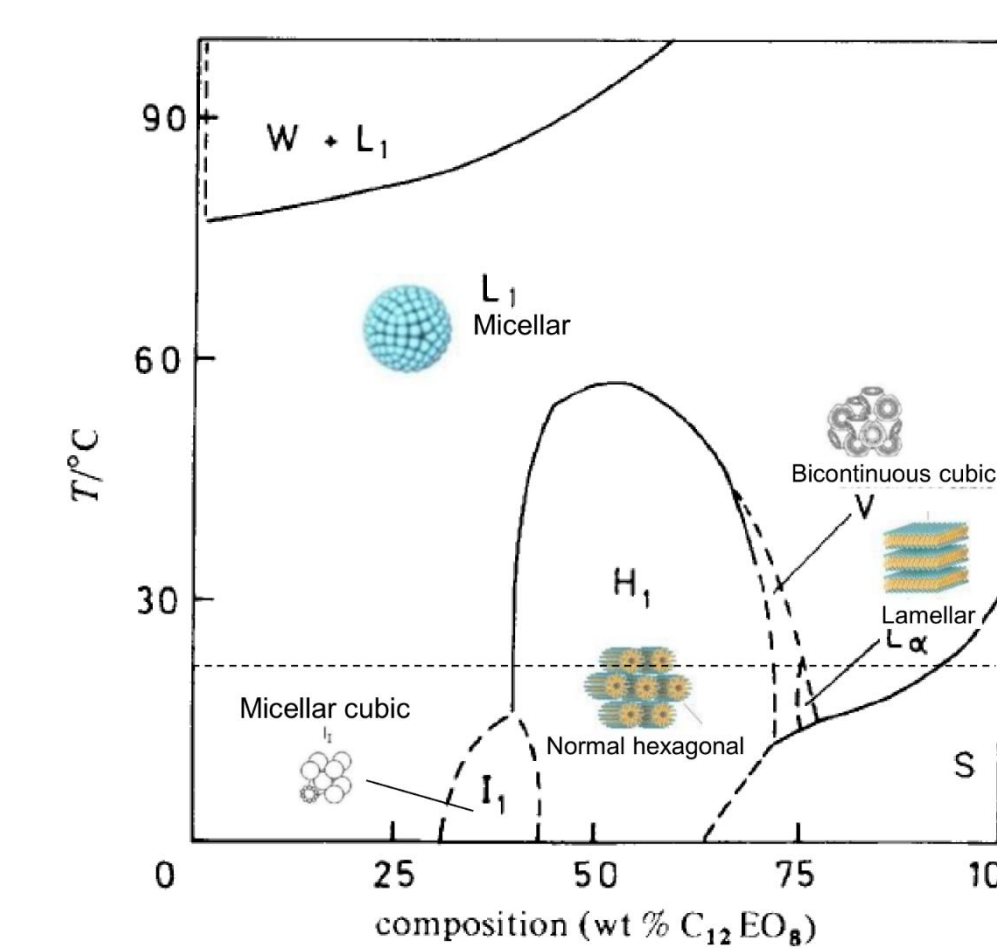


Figure 3. Phase diagram of $C_{12}E_8$ / water system at equilibrium. The diagram is adopted from the literature¹ The dash lines indicate the temperature of our experiments.

1. Schick, M. J., *Nonionic surfactants: physical chemistry*. CRC Press: 1987

B Spreading and retracting of surfactant dissolved droplets

• Spreading

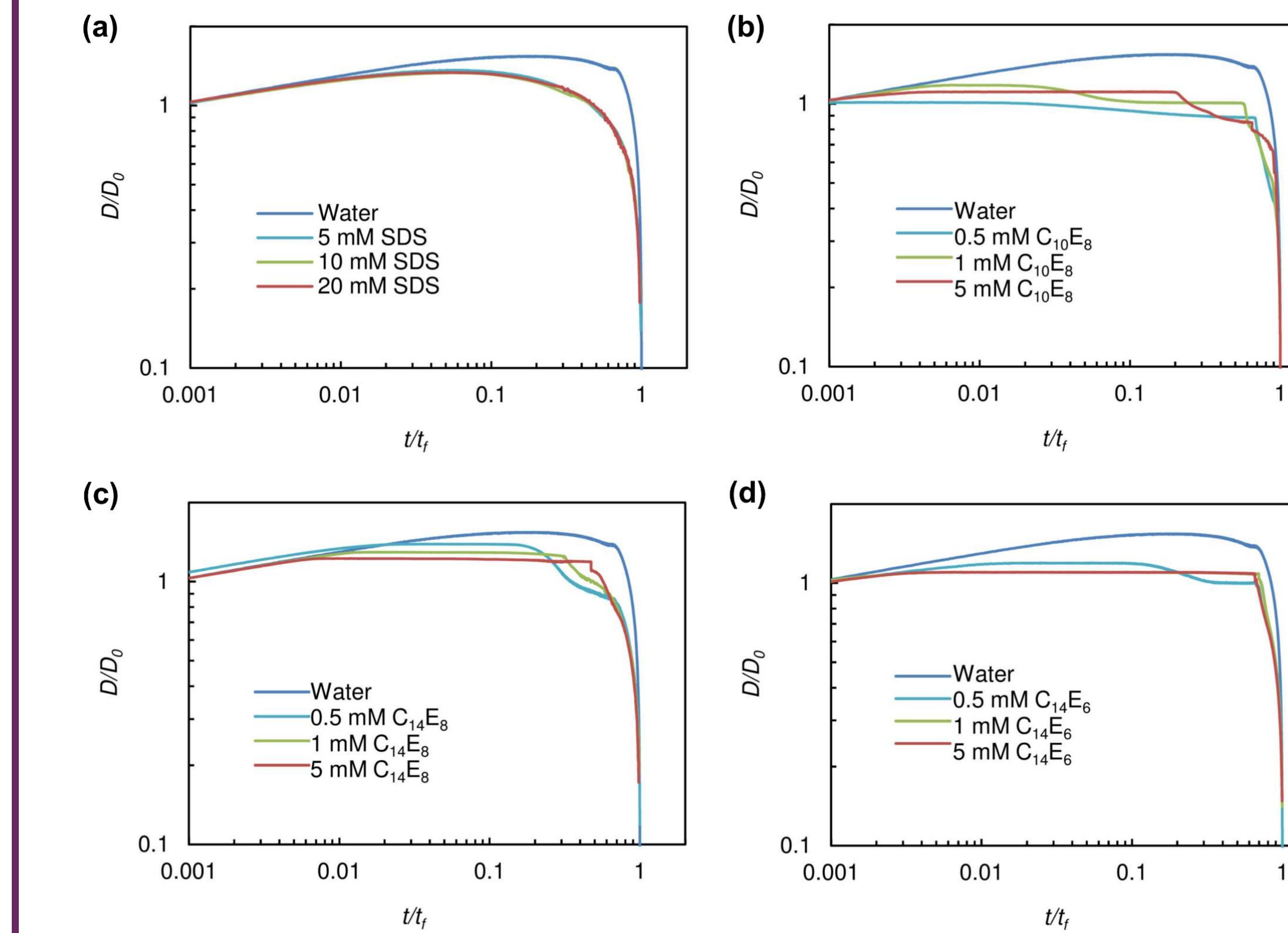


Figure 4. Dimensionless contact diameter versus dimensionless drying time for droplets with different surfactants. D is the diameter of the water (or water-rich) droplet, D_0 the diameter of the droplet upon landing and t_f the vanishing time of the receding droplet, $t_f = O(10^0)$ s. (a) SDS; (b) $C_{10}E_8$; (c) $C_{14}E_8$; (d) $C_{14}E_6$.

- Surprisingly SDS and C_nE_m solutions inhibit spreading on hydrophilic surfaces; the suppressed spreading is more pronounced in C_nE_m solutions. Two possible sources for the suppressed spreading:

- Marangoni contraction
- For C_nE_m -laden droplets, quick formation of a mesophase (liquid crystalline) near the TCL pins the droplets and stops further spreading of the droplets

• Retracting

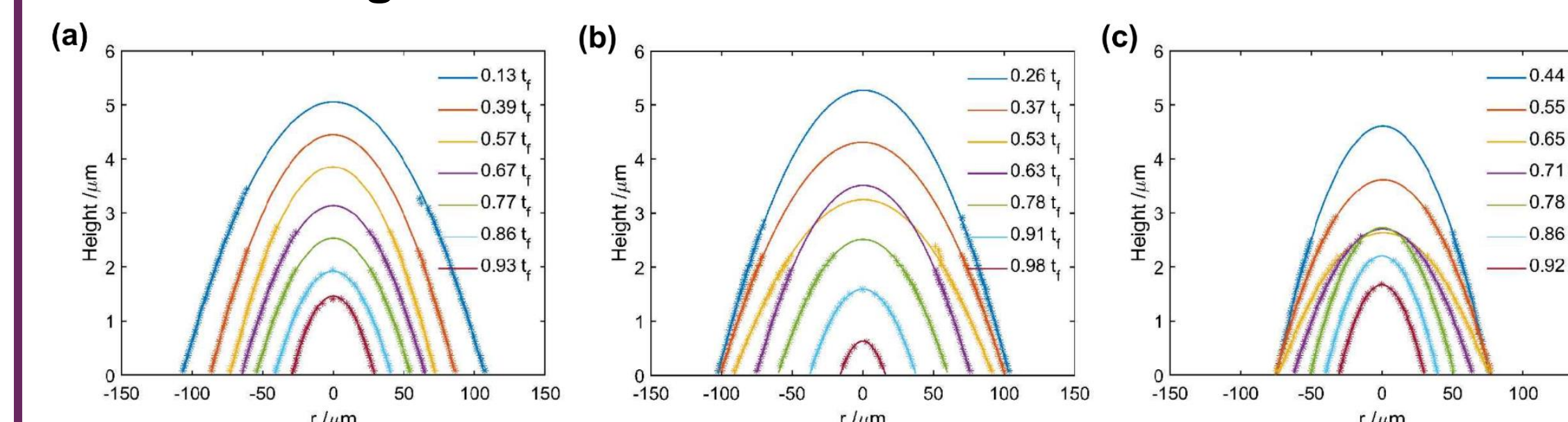


Figure 5. Evolution of height profiles of drying surfactant-laden droplets. The data points are extracted from interference fringes and the lines are spherical caps from curve fitting. t_f denotes the vanishing time of the receding droplet, $t_f = O(10^0)$ s. (a) 5 mM SDS; (b) 5 mM $C_{14}E_8$; (c) 5 mM $C_{14}E_6$.

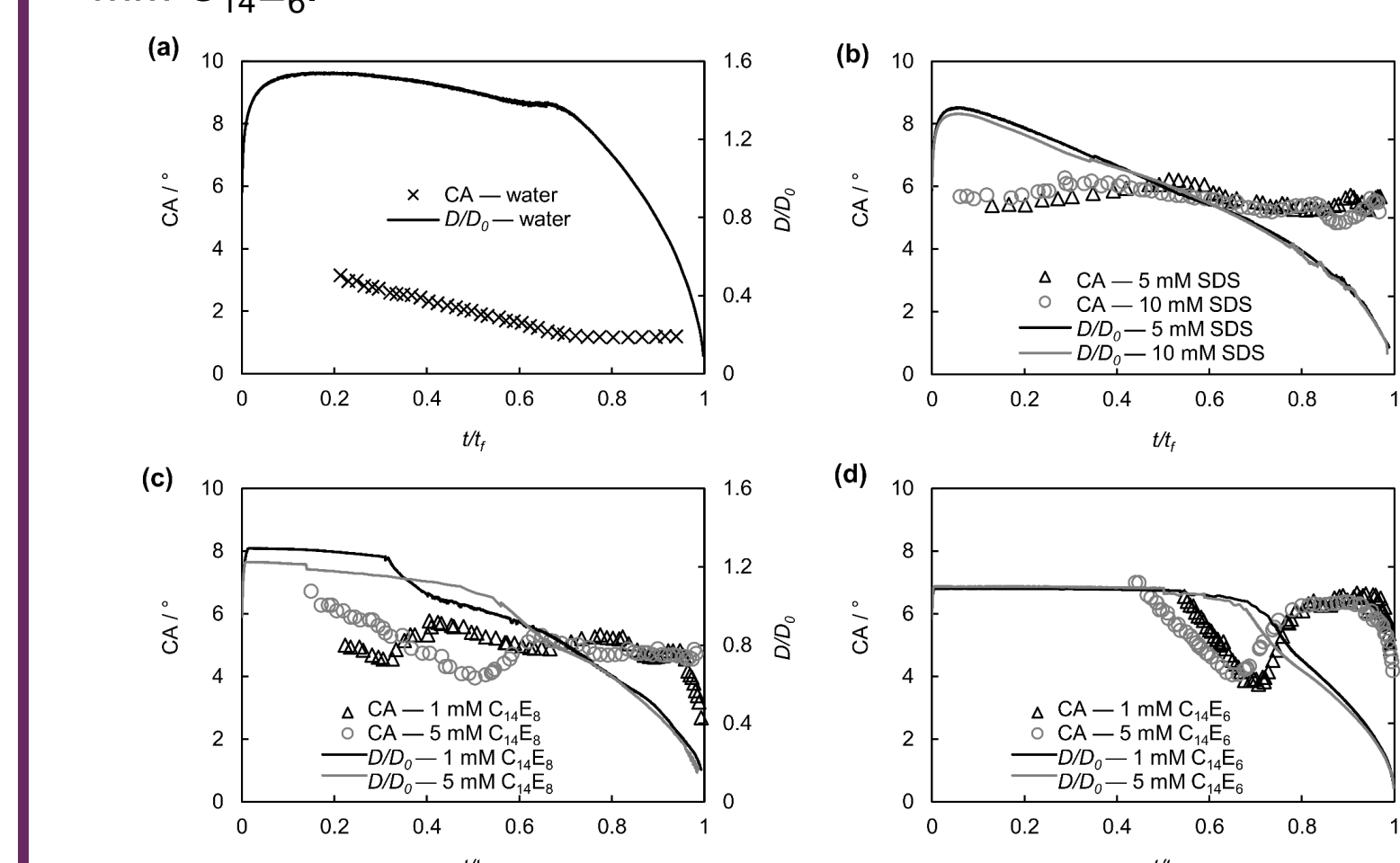


Figure 6. Evolution of the contact angle and contact diameter of a drying water droplet (a) and surfactant-laden (b-d) droplets on a hydrophilic substrate. t_f denotes the vanishing time of the receding droplet, $t_f = O(10^0)$ s.

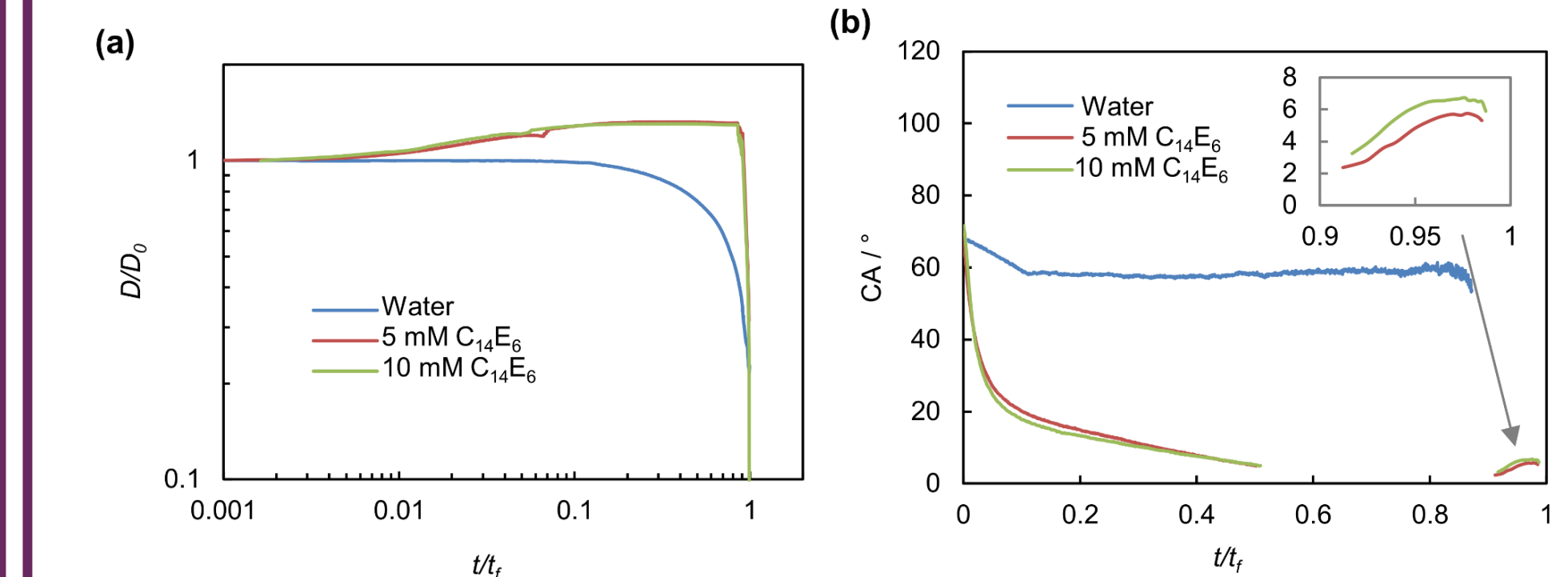


Figure 7. Spreading and retracting (a) and evolution of contact angle (b) of $C_{14}E_8$ -laden droplets on a hydrophobic substrate. t_f denotes the vanishing time of the receding droplet, $t_f=4.0$ s and 4.9 s for droplets with 5 mM and 10 mM $C_{14}E_8$, respectively.

- “Pinning-depinning-jump” behaviour is observed in C_nE_m -laden droplets
- SDS-laden droplets retracts at a constant CA from a very early stage following initial spreading.
- The CA of a C_nE_m -laden droplet first decreases then increases as the droplet depins until the receding contact angle of the water-rich droplet is reached; this CA is independent of hydrophobicity of substrates, supporting the formation of mesophase film at the vicinity of the receding contact line.

C Internal flows during the drying of surfactant dissolved droplets

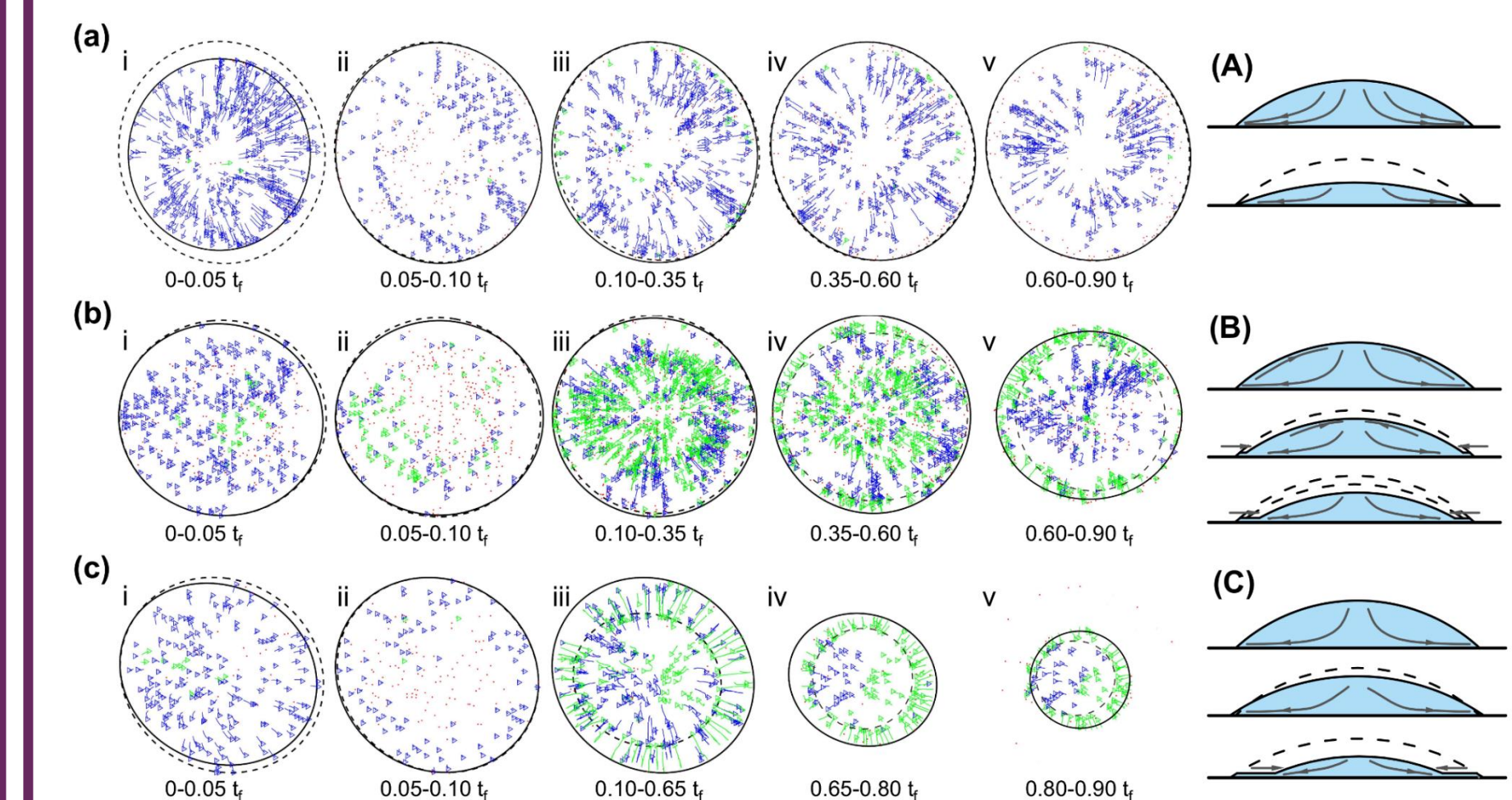


Figure 8. Trajectories of tracer particle (a, b, c) and sketches of internal flows (A, B, C) during the evaporation of C_nE_m -laden droplets containing 0.05 vol % PS particles. (a, A) 0.5 mM $C_{14}E_8$; (b, B) 10 mM $C_{14}E_8$; (c, C) 10 mM $C_{14}E_6$. t_f denotes the vanishing time of the receding droplet, $t_f = O(10^0)$ s. For the trajectories, the red dots represent the stationary particles in the radial direction (movement < three pixels in the time interval), the blue and green lines represent outward and inward trajectories, respectively. The bold line and the dashed line represent the contact line at the start and end of the corresponding time-bin, respectively.

4 Conclusions

- The C_nE_m -laden droplets undergo phase separation with evaporation; phase separation occurs in the priority of the droplet thus a thin mesophase film is left behind a retracting droplet as water evaporates.
- The existence of the mesophase film is corroborated by tests conducted on hydrophobic substrates which showed that the receding contact angle at the late stage of a drying C_nE_m -laden droplet is independent of the hydrophobicity of the substrate.
- Both C_nE_m and SDS solutions inhibit spreading on hydrophilic surfaces, and we attribute this phenomenon to Marangoni contraction. In addition, phase transition at the initial TCL contributes to the more pronounced suppression of droplet spreading for C_nE_m solutions.
- Mild Marangoni flows directing towards the apex exist in droplets with surfactant concentrations well above CMC.

2 Experiments

A Experimental conditions

- Substrates used:
 - Hydrophilic substrate: plasma cleaned glass coverslips, freshly made on the day of experiments.
 - Hydrophobic substrate: HMDS (HexaMethylDiSilazane) treated glass coverslips
- Droplet sizes: 200±50 pL; diameter 200±50 μm (after spreading); drying time of the major droplet $t_f \sim 1$ s
- RH=40%±10%, temperature $T=21\pm0.5$ °C.
- Surfactant concentrations: 0.5, 1, 5, 10 mM for C_nE_m ; 5, 10, 20 mM for SDS.
- Peclet number of micelles: $Pe = \frac{RU}{D} \sim \frac{10^{-4} \times 10^{-4}}{10^{-10}} \sim 100$ (Convection dominant)

B Imaging of the drying process of a droplet

- On Spreading and Drying of Surfactant Droplets
Observed with illumination from underneath the substrate. A high frame rate (4000 fps) was used for tracking the rapid spreading process upon landing of the droplet.
- On Internal Flows During the Drying Of Surfactant Droplets
Droplets of surfactant solutions with 0.04/0.05 vol.% PS tracer particles were observed with oblique illumination.